Fungal Genetics and Biology 94 (2016) 54–68

Contents lists available at ScienceDirect

Fungal Genetics and Biology

journal homepage: www.elsevier.com/locate/yfgbi

Regular Articles

Unh1, an *Ustilago maydis* Ndt80-like protein, controls completion of tumor maturation, teliospore development, and meiosis

Colleen E. Doyle [a], H.Y. Kitty Cheung [a], Kelsey L. Spence [b,1], Barry J. Saville [a,b,*]

[a] Environmental & Life Sciences Graduate Program, Trent University, 1600 West Bank Drive, Peterborough, Ontario K9L 0G2, Canada
[b] Forensic Science Program, Trent University, 1600 West Bank Drive, Peterborough, Ontario K9L 0G2, Canada

ARTICLE INFO

Article history:
Received 14 April 2016
Revised 4 July 2016
Accepted 6 July 2016
Available online 7 July 2016

Keywords:
Ustilago maydis
Plant-induced meiosis
Teliospore maturation
Ndt80-like DNA-binding protein
Melanin biosynthesis

ABSTRACT

In this study, *Ustilago maydis* Ndt80 homolog one, *unh1*, of the obligate sexual pathogen *U. maydis*, is described. Unh1 is the sole Ndt80-like DNA-binding protein in *U. maydis*. In this model basidiomycete, Unh1 plays a role in sexual development, influencing tumor maturation, teliospore development and subsequent meiotic completion. Teliospore formation was reduced in deletion mutants, and those that did form had unpigmented, hyaline cell walls, and germinated without completing meiosis. Constitutively expressing *unh1* in haploid cells resulted in abnormal pigmentation, when grown in both potato dextrose broth and minimal medium, suggesting that pigmentation may be triggered by *unh1* in *U. maydis*. The function of Unh1 in sexual development and pigment production depends on the presence of the Ndt80-like DNA-binding domain, identified within Unh1. In the absence of this domain, or when the binding domain was altered with targeted amino acid changes, ectopic expression of Unh1 failed to complement the *unh1* deletion with regards to pigment production and sexual development. An investigation of *U. maydis* genes with upstream motifs similar to Ndt80 recognition sequences revealed that some have altered transcript levels in Δ*unh1* strains. We propose that the first characterized Ndt80-like DNA-binding protein in a basidiomycete, Unh1, acts as a transcription factor that is required for teliospore maturation and the completion of meiosis in *U. maydis*.

1. Introduction

Ustilago maydis (DC) Corda is an obligate sexual pathogen and the model for biotrophic basidiomycete plant pathogens (Banuett, 1995; Brefort et al., 2009). Its lifecycle consists of three different forms – the haploid saprophytic form, the pathogenic dikaryotic form, and the diploid teliospore (reviewed by Kahmann and Kämper, 2004). Sexually compatible haploids fuse to form the filamentous dikaryon, and at this stage the fungus is an obligate parasite, requiring the plant host for growth and development. The dikaryon invades the plant and grows within and between plant cells, triggering the formation of characteristic tumors (Banuett and Herskowitz, 1996; Martinez-Espinoza et al., 2002; Snetselaar and Mims, 1992). Within these tumors, the branching hyphae fragment into teliospore initials, the initials begin rounding, pigment is deposited and ornamentation occurs leading to darkly pigmented mature teliospores with echinulation (Banuett and Herskowitz, 1996). *U. maydis* teliospores are dormant dispersal agents and the only cell type competent to complete meiosis (Banuett, 1995; Kahmann and Kämper, 2004). Meiosis initiates during the formation of teliospores in the plant, and arrests in late prophase I when the teliospores enter dormancy (Kojic et al., 2013). Following dispersal, teliospores germinate and resume meiosis, completing meiotic divisions and generating haploid cells (Kojic et al., 2013; Saville et al., 2012). Meiosis and teliospore formation are temporally linked in *U. maydis*; however, up to 3% (Christensen, 1931; Kojic et al., 2002), or as high as 10% (Holliday, 1961) of the teliospores fail to complete meiosis and germinate as diploids. Thus, meiosis and teliospore formation are linked but separable events. The obligate *in planta* development required for teliospore formation and meiotic competence indicates the control of these processes in *U. maydis* must respond to signals received while in the plant. This means that part of the key to understanding plant/pathogen interaction during *U. maydis* pathogenesis is elucidating the control pathways that trigger meiosis.

Meiosis is crucial to the maintenance of genetic diversity in all sexually reproducing organisms. The economically important

* Corresponding author at: DNA Building, Trent University, 2140 East Bank Drive, Peterborough, ON K9L 0G2, Canada.
E-mail address: barrysaville@trentu.ca (B.J. Saville).
[1] Present address: Department of Population Medicine, University of Guelph, 50 Stone Road E, Guelph, Ontario N1G 2W1, Canada.

http://dx.doi.org/10.1016/j.fgb.2016.07.006
1087-1845/

smuts and rusts require growth in the host plant to initiate meiosis and this initiation is linked to pathogenic development. In these fungi meiosis is paused at a time analogous to the pachytene checkpoint, or meiotic recombination checkpoint in *Saccharomyces cerevisiae* (Donaldson and Saville, 2008; Kojic et al., 2013; Saville et al., 2012). In *S. cerevisiae* this checkpoint prevents the cell from exiting prophase I and entering into meiotic divisions if recombination has not been completed (Bailis and Roeder, 2000). The progression of meiosis is consistent among sexually reproducing fungi; however, the external cues that induce entry into meiosis and the control of meiotic progression are less conserved (Saville et al., 2012).

A search for *U. maydis* genes potentially involved in meiosis identified *UMAG_02775* (*unh1*) as a probable Ndt80-like transcription factor based upon sequence similarity in the DNA-binding domain (Donaldson and Saville, 2008). These proteins have been characterized in ascomycete fungi where a given species often has multiple Ndt80-like proteins with distinct roles in influencing developmental transitions, including those leading to sexual reproduction (Hutchison and Glass, 2010; Wang et al., 2006). *S. cerevisiae* has a single family member, Ndt80, which is a meiosis-specific transcription factor required for exit from the pachytene checkpoint, leading to meiotic divisions (Chu et al., 1998; Chu and Herskowitz, 1998; Hepworth et al., 1998; Xu et al., 1995). *unh1* has limited sequence similarity to Ndt80-like proteins outside the Ustilaginomycetes, however, its binding domain is conserved. As the only Ndt80-like protein present in *U. maydis*, *unh1* was hypothesized to control progression through meiosis in *U. maydis*. The results of this study support the contention that Unh1 functions as a transcription factor that plays an essential role in sexual development in *U. maydis*, being required for teliospore maturation and the completion of meiosis in *U. maydis*. Therefore, these analyses identify a key component of the largely unknown control pathway for *in planta* teliospore development and meiosis commitment in smut fungi.

2. Materials and methods

2.1. Strain construction and growth conditions

The *U. maydis* strains used in this study are listed in Table 1. Compatible *U. maydis* haploid strains FB1 and FB2 as well as the solo pathogenic diploid strain FB-D12 (Banuett and Herskowitz, 1989) were provided by Flora Banuett (California State University, Long Beach, United States). The haploids were used as wild-type (wt) strains for all experiments. Haploid *U. maydis* cells were grown in YEPS medium (1% yeast extract, 2% sucrose, 2% peptone), potato dextrose broth (PDB; BD Difco), or minimal medium (Holliday, 1974) at 28–30 °C shaking at 250 rpm. Mutants containing the hygromycin resistance cassette were grown on medium supplemented with 300 μg mL^{-1} hygromycin B (BioShop), while those with the carboxin resistance cassette were grown on medium supplemented with 4 μg mL^{-1} carboxin (Sigma). Subcloning efficiency DH5α chemically competent *Escherichia coli* cells (Life Technologies) were transformed with plasmids conferring ampicillin resistance and grown on Lysogeny broth (LB, EMD Millipore) plates or liquid medium (Sambrook and Russell, 2001), containing 100 μg mL^{-1} ampicillin (BioShop), at 37 °C, with liquid cultures shaking at 250 rpm. Plasmids were extracted and purified using the illustra Plasmid Prep Mini Spin Kit (GE Healthcare Life Sciences). Ligations for vector construction were carried out with T4 DNA ligase (New England Biolabs) and incubated at 16 °C for 21 h. To verify correct vector construction, the inserted fragments were sequenced from the plasmid using Big Dye Terminator chemistry V3.1 (ABI) and an automated sequencer (ABI 3730 DNA analyzer). Raw sequences were trimmed using default settings of the SeqManII module of Lasergene v.5.0 (DNASTAR), and aligned using MEGA 5 (Tamura et al., 2011).

The *U. maydis unh1* deletion constructs were created following the PCR-based method established by Kämper (2004). *E. coli* containing plasmids pMF1-c (carboxin resistance) and pMF1-h (hygromycin resistance) (Brachmann et al., 2004), were obtained from Jörg Kämper (Karlsruhe Institute of Technology, Karlsruhe, Germany). The 5′ and 3′ regions flanking the *unh1* gene were amplified from genomic DNA by PCR using Finnzymes Phusion according to the manufacturer's suggested protocol (Thermo Fischer Scientific). The 5′ and 3′ flanking regions of the genes were amplified with primers *unh1*_LF_Out-F and *unh1*_LF_SfiI-R and *unh1*_RF_Out-R and *unh1*_RF_SfiI-F (Table S1), respectively. The products were purified using the QIAquick Gel Extraction Kit (Qiagen) following the microcentrifuge protocol. The flanking regions were digested with *Sfi*I; pMF1-h and pMF1-c were digested with *Sfi*I and *Bsa*I (New England Biolabs). The digested products were purified by gel extraction. DNA concentration was determined using a Nanodrop 8000 Spectrophotometer (Thermo Scientific) and equal concentrations of each flank were ligated to either the hygromycin B or carboxin cassette. The ligation product was gel extracted and amplified by PCR with Finnzymes Phusion using the nested primers, *unh1*_LF_Nest-F and *unh1*_RF_Nest-R (Table S1). The hygromycin B resistance construct was transformed into FB1 and the carboxin resistance construct was transformed into FB2, replacing *unh1* by homologous recombination. Transformation was carried out by the method of Wang et al. (1988), as modified in Morrison et al. (2012). This resulted in the creation of the deletion strains FB1Δ*unh1* and FB2Δ*unh1* (Table 1). Integration of the construct at the *unh1* locus was confirmed through PCR and Southern blot analysis using the DIG High Prime DNA labeling and Detection Starter Kit 1 (Roche). The absence of *unh1* transcripts in the deletion mutants was assessed by RT-PCR using primers Unh1-F and Unh1-R (Table S1).

The *unh1* deletion was complemented with wild-type *unh1* (p*unh1*), *unh1* with residues K641 through A824 deleted (p*unh1*ΔKA) and *unh1* containing R to A point mutations at residues 647, 720 and 761 (p*unh1*3A). *U. maydis* strains p*unh1*, p*unh1*ΔKA and p*unh1*3A were created in the FB1 Δ*unh1* strain. The wild-type *unh1* gene was obtained by amplification of cDNA isolated from *U. maydis* teliospores with the primers PublexUnh1-F and PublexUnh1-R (Table S1) using Platinum Taq

Table 1
Strains used in this study.

Name	Strain	Relevant genotype[a]	Source
Wild-type (wt)	FB1	*a1 b1*	Banuett and Herskowitz (1989)
	FB2	*a2 b2*	Banuett and Herskowitz (1989)
Solopathogenic diploid	FB-D12	*a1/a2 b1/b2 pan−/+ ade −/+*	Banuett and Herskowitz (1989)
Δ*unh1*	FB1Δ*unh1*	*a1 b1* Δ*unh1*::*hph*	This publication
	FB2Δ*unh1*	*a2 b2* Δ*unh1*::*carbR*	This publication
p*unh1*	FB1Δ*unh1* otef: *unh1*	*a1 b1* Δ*unh1*::*hph* otef: *unh1*::*carbR*	This publication
p*unh1*ΔKA	FB1Δ*unh1* otef: $unh1^{\Delta 641-824}$	*a1 b1* Δ*unh1*::*hph* otef: $unh1^{\Delta 641-824}$::*carbR*	This publication
p*unh1*3A	FB1Δ*unh1* otef: $unh1^{RA647,720,761}$	*a1 b1* Δ*unh1*::*hph* otef: $unh1^{RA647,\ 720,\ 761}$:: *carbR*	This publication

[a] unh1 is UMAG_02775.

DNA Polymerase (Life Technologies). This fragment was 2802 bp long and was cloned into the Publex Integrating plasmid, obtained from Guus Bakkeren (Agriculture and Agri-Food Canada, Summerland, Canada) by digesting the amplified gene fragment with *Bam*HI and the plasmid with *Bgl*II (New England Biolabs). Plasmids containing p*unh1*ΔKA and p*unh1*3A, were obtained in pUC57 plasmids (synthesized by GenScript). To construct plasmids to express p*unh1*, p*unh1*ΔKA and p*unh1*3A in *U. maydis*, the entire open reading frame was amplified from the pUC57 plasmids by PCR using the primers Unh1XmaI-F and Unh1NotI-R and Elongase enzyme (Life Technologies; Table S1). These fragments were digested with *Xma*I and *Not*I (New England Biolabs) and cloned into the p123 plasmid, obtained from Jörg Kämper (University of Karlsruhe, Karlsruhe, Germany). p123 is an integrative *U. maydis* vector that contains an otef promoter, to allow the constitutive expression of a gene in *U. maydis* (Basse et al., 2000); it was digested with *Xma*I and *Not*I and purified by gel extraction to excise eGFP and allow for insertion of the native and modified *unh1* ORFs. The resulting plasmids were linearized by *Ssp*I digestion (New England Biolabs) and integrated at the *ip* locus of the Δ*unh1* strain by homologous recombination. The integration at the *ip* locus was verified by PCR and Southern blot analysis. Expression of the gene was confirmed through RT-PCR using RNA isolated from axenic cultures.

2.2. RNA isolation, RT-PCR and RT-qPCR

Gene sequences for primer design were obtained from MIPS *U. maydis* Database (MUMDB; http://mips.helmholtz-muenchen.de/genre/proj/ustilago/, accessed 2012). Primers were designed using Primer3 (Rozen and Skaletsky, 2000). Primers designed for RT-PCR are listed in Tables S2 and S3. Total RNA was extracted using TRIzol reagent (Invitrogen). Haploids were grown in PDB for 24 or 48 h, then centrifuged at 5250*g* for 20 min at 4 °C. The pellet was washed in 50 mL of diethylpyrocarbonate (DEPC) treated water and centrifuged. RNA isolation was then completed as per Morrison et al. (2012). Dried teliospores (~50–100 mg) were suspended in up to 3 mL of TRIzol and transferred to Lysing Matrix C tubes and disrupted with a FastPrep-24 set at 6.5 m s^{-1} for 45 s. Disruption was carried out three times, with 1 min incubation on ice in between. After this step, RNA isolation proceeded as per Morrison et al. (2012). Following isolation, 1–10 μg of total RNA was treated with DNaseI (RNase-free, New England Biolabs), precipitated, re-suspended in DEPC-treated water and stored at −80 °C. RNA was quantified with a Nanodrop 8000 (Thermo Scientific). DNaseI treated total RNA was assessed for genomic contamination as in Morrison et al. (2012). Reverse transcription using the ABI TaqMan Gold RT-PCR kit (ABI) was carried out in a 10 μL reaction volume, using DNaseI treated total RNA, primed with oligo-d $(T)_{16}$. Subsequently, PCR was carried out in 25 μL reactions with Amplitaq Gold DNA Polymerase (Applied Biosystems). The cycling conditions of the amplifications were: 95 °C for 10 min, then 30 cycles of 95 °C for 30 s, 63 °C for 15 s and 72 °C for 30 s, then 72 °C for 10 min with a 4 °C hold at the end. PCR products were visualized under UV light following electrophoretic separation on an agarose gel containing 0.3 μg mL^{-1} ethidium bromide (BioShop). Transcript levels were compared to those of the housekeeping gene *UMAG_02491* (*gapd*, glyceraldehyde 3-phosphate dehydrogenase).

RT-qPCR primers and TaqMan probes were designed using Primer Express Software version 2.0 (Applied Biosystems) using default criteria, for 13 genes (Table S4). Previous work led to the selection of *UMAG_00175* as the endogenous control gene for dormant teliospore analysis (Morrison et al., 2012; Seto, 2013). RT-qPCR was carried out using the StepOne Plus Real-Time PCR System (Applied Biosystems), with a 10 μL TaqMan Universal PCR Master Mix (Life Technologies) reaction. The cycling conditions used were: 50 °C for 2 min, 95 °C for 10 min followed by 40 cycles of 95 °C for 15 s and 60 °C for 1 min. The data was collected and analyzed using StepOne Plus software (Applied Biosystems). The results were analyzed using comparative C_T ($2_T^{-\Delta\Delta C}$) method, with *UMAG_00175* as the endogenous control and wild-type teliospore cDNA as the calibrator.

2.3. Pathogenesis assays, corn infection and sampling

Assessments of pathogenesis were carried out using a corn seedling assay as outlined by Morrison et al. (2012). Symptoms were scored according to a 0–6 disease scoring scale modified from that described previously by Gold et al. (1997) and Kämper et al. (2006). Briefly, disease ratings included: 0 = no symptoms; 1 = anthocyanin production and/or chlorosis; 2 = small leaf tumors; 3 = small stem tumors; 4 = large stem tumors; 5 = large stem tumors with stem bending and 6 = plant death. Plants were scored at 7, 10, 14, and 21 days post infection (dpi). For microscopic analysis of plant infection, seedlings were grown and scored as above and were selected if they were considered to be an average representation of all infected plants. Tissue was prepared based on a modification of the procedure described in Banuett and Herskowitz (1996). Free hand cross-sections of sampled plant tissue were prepared for microscopy using double-edged, uncoated razors (American Safety Razor Company) and transferred to a glass slide using a nylon paint brush (Daler-Rowney Ltd.) for microscopic observation.

The infection of corn cobs for the isolation of teliospores, Golden Bantam (Ontario Seed Company) was carried out on plants grown and detasseled, as described in Morrison et al. (2012). After the appearance of silks on the corn cobs, they were infected using *U. maydis* culture diluted to an OD_{600} of 1 as determined with a GENESYS 10S UV–vis Spectrophotometer (Thermo Scientific). 6 mL of culture, containing equal concentrations of compatible haploid cells was injected down the silk shaft of each cob with a 10 mL syringe and 18 gauge needle.

2.4. Teliospore isolation, germination and segregation of resistance

Approximately 28–35 dpi, cobs were removed from the stalks and the mature tumors were collected. Teliospores were isolated using a modification of the Zahiri et al. (2005) procedure. Briefly, harvested tumors were ground in a Waring blender and the suspension was filtered through four layers of cheese cloth. The filtrate was transferred to a 250 mL bottle and centrifuged at 1000*g* for 10 min in an Allegra X-15R centrifuge (Beckman Coulter). The supernatant was decanted and the teliospore pellet was washed in sterile water, transferred to a sterile 50 mL Falcon tube and washed three more times with centrifugation at 1000*g* for 5 min between each wash. This was followed by 5–8 additional washes with centrifugation at 600*g* for 5 min between each wash. The supernatant was decanted and the light brown layer on top of the pellet, containing plant material, was removed. The washed teliospores were dried in a vacuum desiccator (Nalgene) then stored at 4 °C.

To induce germination, dried teliospores were re-suspended in sterile water and 0.75% $CuSO_4$ solution and agitated for 3 h. They were then centrifuged at 2500*g* for 5 min, the $CuSO_4$ was removed and the pellet was rinsed 3 times with sterile water and spread on YEPS plates with 160 μg mL^{-1} streptomycin and 50 μg mL^{-1} kanamycin (BioShop) and incubated at 28 °C for 20–24 h. The plates were then rinsed with sterile water and cells were quantified in the resulting suspension using a haemocytometer, then diluted to 1000 cells mL^{-1} with sterile water. 100 μL of this cell suspension was spread on fresh YEPS plates containing streptomycin and kanamycin and incubated at 28 °C, until single colonies were

apparent (approximately 2 days). To assess segregation of resistance, single colonies from this germination were patched onto YEPS plates containing selection (300 μg mL^{-1} of hygromycin B or 4 μg mL^{-1} of carboxin). The growth of each colony on each type of selection was recorded. This was repeated three times for each colony, to ensure correct assessment of resistance. To test for the ability of putative diploid progeny to grow filamentously, single colonies were struck out onto nutrient medium containing charcoal (DCM or PD) and the appearance of filamentous growth, the Fuz^+ phenotype (Holliday, 1974) was recorded.

2.5. Microscopy

Microscopic observations were carried out with a Zeiss AxioScope.A1 microscope with DIC contrast. Micrographs were taken with a Zeiss AxioCam ICc1 for color photographs and Zeiss AxioCam ICm1 for black and white photographs, using the Zen 2011 software (Zeiss). Mature teliospores were suspended in water, 10 μL of the suspensions were placed on a 75 × 25 × 1 mm glass slide (VWR) and covered with an 18 × 18 mm glass coverslip (VWR) for observation. For haploid cells grown in liquid medium, a 10 μL drop of culture was placed on a slide, covered and observed. For *in planta* growth assays, cross-sections of plant tissue were mounted in a drop of water and covered. After mucilaginous matrix formation, at 9 dpi, samples were gently pressed down before observation, as described by Banuett and Herskowitz (1996), for a clearer observation of hyphal cells.

2.6. Bioinformatic analysis

For alignment to Unh1, additional fungal Ndt80-like DNA-binding domain (DBD) proteins were identified from Pfam (Finn et al., 2014). The DBD for each protein was then identified using NCBI BLAST (Altschul et al., 1990). The DNA-binding domains were aligned using MAFFT (Goujon et al., 2010; Katoh and Toh, 2008; McWilliam et al., 2013) and visualized using Jalview (Waterhouse et al., 2009). The aligned protein binding domains were used to generate a Bayesian phylogenetic tree using the LG + G amino acid substitution model, estimated by ProtTest 3 (Darriba et al., 2011; Guindon and Gascuel, 2003) in MRBAYES 3.2 (Huelsenbeck and Ronquist, 2001; Ronquist and Huelsenbeck, 2003), with 4 chains run for 2 million generations with a sample frequency of 200 and a 25% burn-in. Trees were visualized using FigTree (http://tree.bio.ed.ac.uk/software/figtree/).

Using the program DNA Pattern Find (Stothard, 2000), the upstream regions of 3246 *U. maydis* genes were searched for motifs with similarity to the well characterized DNA sequence binding site for an Ndt80-like protein, the middle sporulation element (MSE) from *S. cerevisiae*, gNCRCAAAW. For 2977 of these genes, full-length transcript data was available so the starts of transcription were known, and the region up to 1000 bp upstream from this was examined. The additional 269 were other, meiosis related genes, based on FUNCAT designation (MIPS) or previous work (Donaldson and Saville, 2008). No full-length transcript data were available for these genes so regions up to 1500 bp upstream of the start of translation, but not overlapping with adjacent genes, were examined. All instances of a canonical MSE or a less stringent variant (GNCRCNNNN) were recorded.

The program MEME, which identifies novel motifs in nucleotide sequences (Bailey and Elkan, 1994) was used to analyze the upstream region (as defined above) of genes with altered expression confirmed by RT-qPCR, to search for sequence similarities between them. It was set to identify up to 10 motifs, any number of repetitions, with a width of between 6 and 20 bp. Identified motifs were run through TOMTOM, which compares these to known motifs (Gupta et al., 2007) for comparison to the JASPAR (Bryne et al., 2008) core 2009 database, which is a database of published transcription factor binding sites. Known motifs with similarity to those identified by MEME were found.

3. Results

3.1. Unh1 is not required for mating and pathogenesis

The ability of Δ*unh1* strains to mate was tested by co-spotting compatible haploid strains on charcoal-containing solid medium and observing the appearance of the Fuz^+ phenotype (Banuett and Herskowitz, 1989). Co-spotting of either Δ*unh1* × wt or Δ*unh1* × Δ*unh1*, resulted in filamentous growth. This indicated that mating was unaffected by the deletion of *unh1* (Fig. S1).

The pathogenicity of the Δ*unh1* mutants was assessed by infecting corn seedlings with pairs of sexually compatible strains: Δ*unh1* × Δ*unh1*, Δ*unh1* × wt, or wt × wt. The Δ*unh1* strains showed no signs of diminished virulence, whether they were crossed with one another or with wild-type strains (Fig. S2). Kruskal-Wallis tests showed that the resulting plant infections had indistinguishable rates of infection, symptom development, tumor formation, and plant death at 14 dpi ($p > 0.05$, $n = 2$). This indicates that *unh1* is not required for pathogenicity. However, in the later stages of the infection, a phenotypic difference was noted between the wild-type infections and the Δ*unh1* × Δ*unh1* infections. As they matured, tumors formed by the wild-type infections, as well as those formed by Δ*unh1* × wt infections, began to darken in color,[2] turning characteristically grey/black in appearance. However, the infection with compatible Δ*unh1* strains resulted in pale tumors which, developed a light brown/beige coloration, and retained this color for the duration of the infection. In cob infections, bisection of the tumors revealed that the interior of the wt × wt and Δ*unh1* × wt infections were filled with dark, dusty teliospores (Fig. 1A and B); whereas, the tumors of Δ*unh1* × Δ*unh1* infections had fewer, light-colored teliospores (Fig. 1D). This indicated that the deletion of *unh1* resulted in defects in teliospore maturation.

3.2. Unh1 is required for teliospore formation and pigmentation

Microscopic analyses of teliospore formation in seedlings infected with compatible wild-type strains or compatible Δ*unh1* strains, revealed that the early stages of infection and pathogenic development were indistinguishable. Between 6 and 8 dpi, hyphal filaments with branching primordia were observed in both infections, and the initiation of fragmentation occurred at the end of this period (Fig. 2A and E). After this stage, variation was observed between the wt × wt and Δ*unh1* × Δ*unh1* infections. Between 9 and 11 dpi, rounded hyphal cells and immature teliospores were observed in the wild-type infections (Fig. 2B), while Δ*unh1* × Δ*unh1* infections showed hyphal fragmentation and some initial cell rounding but no immature teliospores (Fig. 2F). From 12 dpi onward, mature teliospores were observed in the wild-type infections; the teliospores were darkly pigmented, roughly spherical and had echinulated cell walls (Fig. 2C). The Δ*unh1* × Δ*unh1* teliospores did not further develop, but remained immature. They appeared oblong, pale and smooth, and lacked the typical echinulation seen on wild-type teliospores (Fig. 2G). For the remainder of the time-course, in the wild-type infection, the number of mature teliospores increased in quantity, becoming apparent without magnification (Fig. 2D). Conversely, the quantity of Δ*unh1* × Δ*unh1* teliospores, did not increase markedly over the course of the infection. The end result was rare, scattered, immature teliospores, even late in the infection (Fig. 2H). Overall, the

[2] For interpretation of color in Figs. 1, 3 and 5, the reader is referred to the web version of this article.

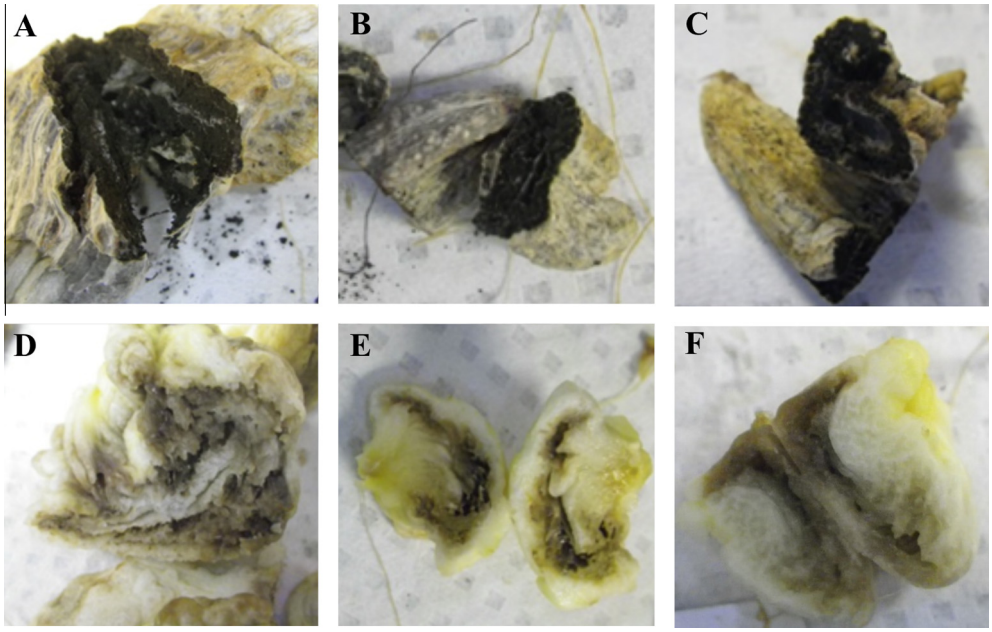

Fig. 1. Deletion or mutation of *unh1* alters maturation of *U. maydis* tumors. Bisected tumors showing teliospores formed from infections of corn cobs with *U. maydis* strains: (A) wt × wt, (B) wt × Δ*unh1*, (C) p*unh1* × Δ*unh1*, (D) Δ*unh1* × Δ*unh1*, (E) p*unh1*ΔKA × Δ*unh1*, and (F) p*unh1*3A × Δ*unh1*.

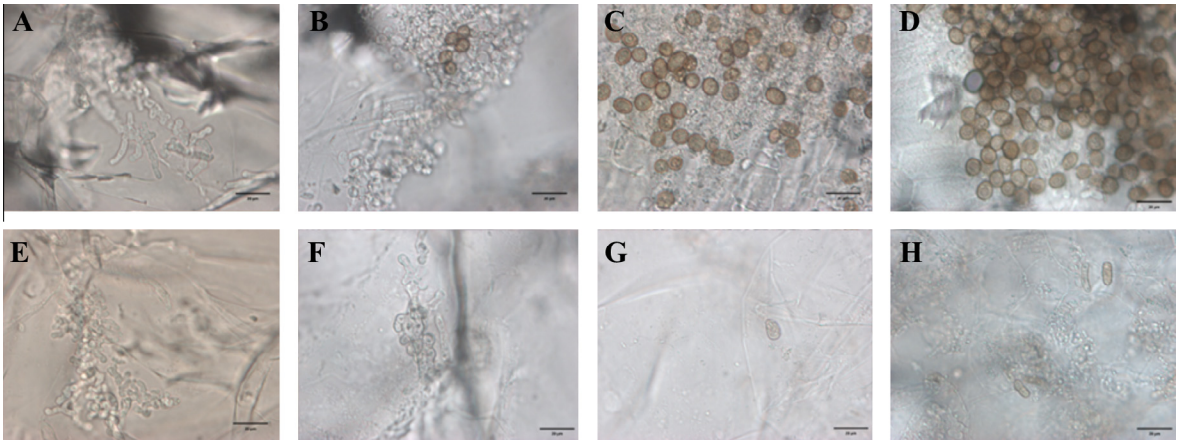

Fig. 2. Teliospore development and maturation is affected by the deletion of *unh1*. Micrographs of teliospore development in corn seedlings (400×). wt × wt: (A) 8 DPI, (B) 10 DPI, (C) 14DPI, (D) 21 DPI. Δ*unh1* × Δ*unh1*: (E) 8 DPI, (F) 10 DPI, (G) 14DPI, (H) 21 DPI. Scale bar indicates 20 μm.

observed *in planta* development mirrored the macroscopically assessed pathogenic symptoms, with the Δ*unh1* × Δ*unh1* infection developing normally initially, resulting in the typical pathogenic symptoms and tumor formation. However, at the stage where teliospore formation and maturation began, the Δ*unh1* × Δ*unh1* infection failed to form mature, pigmented teliospores, resulting in the pale tumors that were observed.

The same phenotype was observed in teliospores isolated from mature corn cob infections. That is, wild-type infections resulted in darkly pigmented teliospores with pronounced echinulation (Fig. 3A). Δ*unh1* × Δ*unh1* teliospores, remained pale and smooth, lacking echinulation and dense pigmentation (Fig. 3B). Despite the observed phenotypic differences, Δ*unh1* × Δ*unh1* and wild-type teliospores both germinated and formed promycelia (Fig. 3C and D). As such, although teliospore formation and maturation were clearly disrupted by the deletion of *unh1*, the abnormal teliospores produced were still viable. Analysis of meiotic completion identified further differences between the wild-type and Δ*unh1* × Δ*unh1* teliospores.

3.3. Completion of meiosis and formation of haploid progeny requires *unh1*

Infecting cobs with compatible Δ*unh1* strains created with distinct selectable markers allowed meiotic segregation to be assessed by replica plating the products of teliospore germination on appropriate antimycotics. Teliospores isolated from the wt × Δ*unh1* infections were phenotypically normal and segregated for antimycotic resistance (Table 2). Teliospores isolated from the Δ*unh1* × Δ*unh1* infections, which were smooth and not echinulated (Fig. 3C and D), showed a severe deficiency in segregation. 89.6% grew on both hygromycin and carboxin (Table 2). χ^2 tests revealed that the observed segregation of Δ*unh1* × Δ*unh1* teliospores is significantly different than expected if meiosis was occurring normally. Note that the expected numbers for χ^2 were conservatively based upon a 3% failure rate of meiosis (Table 2). However, segregation of the wt × Δ*unh1* was consistent with what was expected (χ^2, $p > 0.05$). The majority of progeny resulting from Δ*unh1* × Δ*unh1* teliospore germination also grew as filaments on

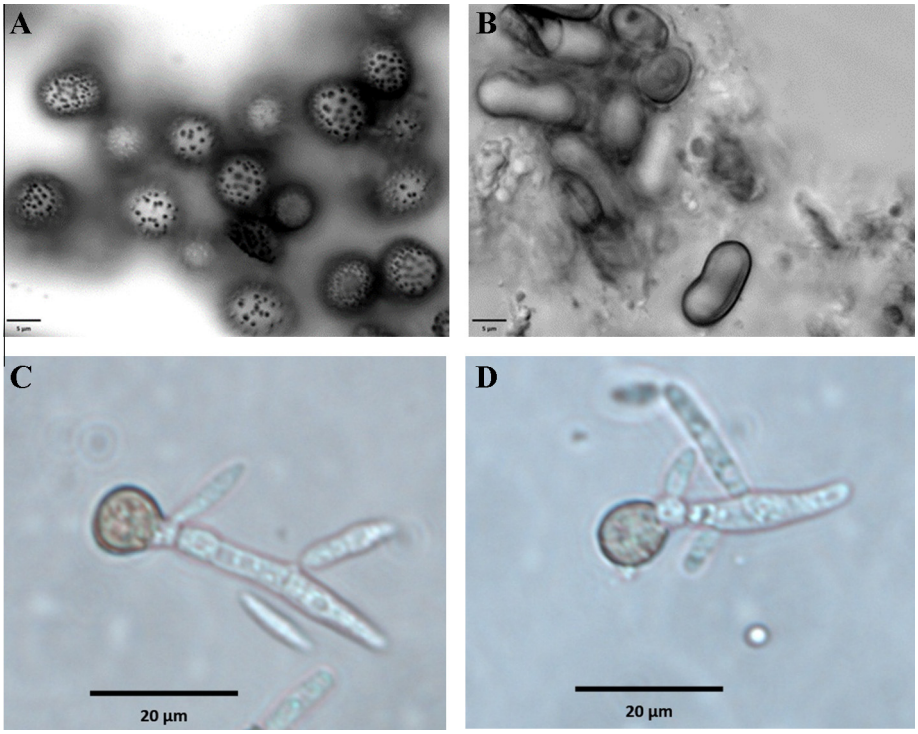

Fig. 3. *unh1* deletion alters teliospore maturation and ornamentation, but not viability. (A) wt × wt, and (B) Δ*unh1* × Δ*unh1*, are black and white micrographs of teliospores harvested from mature corn cob infections (1000×). Scale bar indicates 5 µm. (C) wt × wt, and (D) Δ*unh1* × Δ*unh1*, are micrographs of teliospores germinated on YEPS plates for 24 h (400×). Scale bar indicates 20 µm.

Table 2
Segregation of resistance in colonies from germinated teliospores.

Sample	Colonies	Expected segregation if meiosis occurred			Observed segregation			
		Carb[a] (%)	Hyg[b] (%)	Both (%)	Carb[a] (%)	Hyg[b] (%)	Both (%)	Filamentous growth %
Δ*unh1* × wt[c]	104	0	53	0	0.0	49.0	0.0	2.9
wt × Δ*unh1*[c]	83	53	0	0	61.4	0.0	0.0	10.8
Δ*unh1* × Δ*unh1*[d]	201	48.5	48.5	3	9.0	1.5	89.6	85.6
p*unh1* × Δ*unh1*[d]	624	48.5	23.5	28	42.5	29.8	27.7	7.2
p*unh1*ΔKA × Δ*unh1*[d]	99	48.5	23.5	28	4.0	0	96.0	75.8
p*unh1*3A × Δ*unh1*[d]	216	48.5	23.5	28	2.8	0.5	96.8	71.3

[a] Carboxin antimycotic resistant.
[b] Hygromycin B antimycotic resistant.
[c] χ^2 tests indicated that results were not significantly different from expected.
[d] χ^2 tests indicated that results were significant different from expected.

charcoal plates, suggesting that they were diploids, not haploids (Table 2). This result was replicated with teliospores that had been treated with $CuSO_4$, confirming that the germinating teliospores were severely deficient in meiosis completion when *unh1* was deleted. Note that there was no growth on plates when haploid cultures were treated with CuSO4 in the same way that teliospores were treated. Plates were left for one week and, while untreated cells formed a lawn, treated cells did not grow (data not shown). A pathogenesis assay conducted using three progeny of Δ*unh1* × Δ*unh1* teliospores showed that they were each able to infect the plant and form tumors without the need for a mating partner (Fig. S3). The degree of symptom formation was less than that of a dikaryon infection, but equivalent to that of the diploid solopathogen, FB-D12 (Kruskal-Wallis test and Dunn multiple comparison, $p > 0.05$). This supports the conclusion that teliospores formed by crosses of Δ*unh1* strains germinated without completing meiosis to form diploid progeny.

3.4. Complementation of unh1 restores wild-type phenotype

In order to confirm that the phenotype of the deletion strains was the result of *unh1* loss, complementation strains were created by inserting *unh1* at the *ip* locus (Basse et al., 2000). When the complemented strains (p*unh1*) were crossed with sexually compatible Δ*unh1* strains during cob infections, the tumors formed were the typical grey/black color of wild-type (Fig. 1C). The teliospores of the complemented strains (Fig. 4C) were also typical of those produced by wild-type strains (Fig. 4A). They were darkly pigmented and echinulated although the echinulation were slightly less pronounced than wild-type. In contrast the Δ*unh1* × Δ*unh1* teliospores (Fig. 4B) were pale and smooth-walled.

Germination of the teliospores formed by the complemented strains was also assessed. Complementation of Δ*unh1* resulted in the formation of strains that contain the carboxin and hygromycin resistance genes at the *ip* locus and *unh1* loci, respectively. These

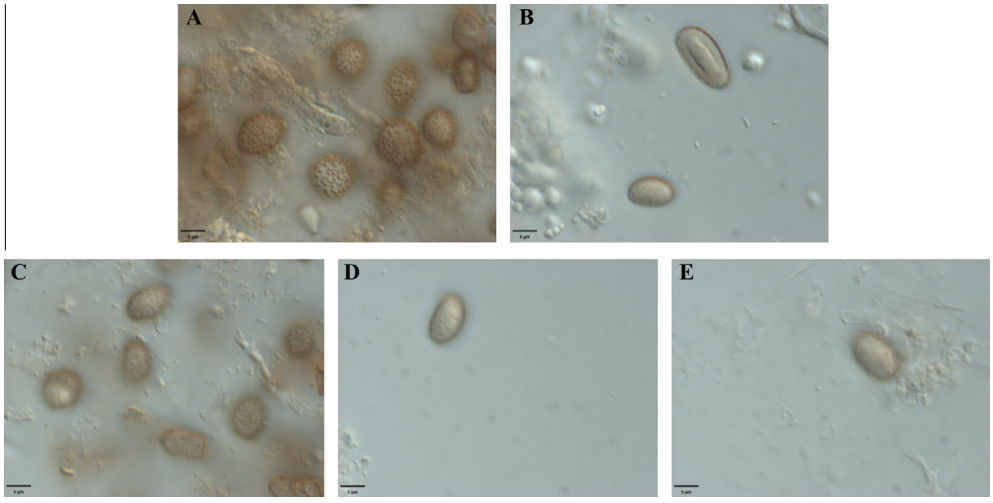

Fig. 4. Unh1 with an altered DBD fails to complement the teliospore maturation defect of Δ*unh1*. Color micrographs of teliospores harvested from mature corn cobs infected with *U. maydis* strains (1000×): (A) wt × Δ*unh1*, (B) Δ*unh1* × Δ*unh1*, (C) p*unh1* × Δ*unh1*, (D) p*unh1*ΔKA × Δ*unh1*, and (E) p*unh1*3A × Δ*unh1*. Scale bar indicates 5 μm. (For interpretation of the references to color in this figure legend, the reader is referred to the web version of this article.)

loci are on different chromosomes, and with the complementation (p*unh1* × Δ*unh1* cross) segregation is restored (Table 2). The observed growth on the antimycotic agent indicates that the re-introduction of *unh1* into the Δ*unh1* strain resulted in the restoration of wild-type teliospore formation and maturation, as well as meiotic completion.

The haploid p*unh1* complementation strains were indistinguishable from wild-type when grown in YEPS medium; however, when grown in PDB, cultures of these strains changed from the typical peach/beige to a dark brown color. Microscopic observation of these cultures revealed that, while the p*unh1* haploid cells were initially typically cigar shaped (Fig. 5A), they became irregularly spherical and pigmented after 2–3 days in culture. These cells also clumped together, while the other strains did not. The pigmentation darkened as culture time was increased, resulting in cells that were obviously spherical and darkly pigmented (Fig. 5E). Cells of wild-type cultures remained cigar shaped and unpigmented when similarly grown (Fig. 5A). The p*unh1* strains have higher *unh1* transcript levels than wild-type haploid strains (Fig. S4). This suggested that the observed pigmentation and rounding of the cells is due, in part, to the increased expression of *unh1*. An attempt to link these processes was made by determining the transcript levels of putative melanin biosynthesis genes in wild-type and complemented p*unh1* strains. RT-PCR results revealed that the predicted laccases, *UMAG_05361* (*lac1*) and *UMAG_05861* (*lac2*), and the predicted tyrosinases, *UMAG_01130* and *UMAG_10756* had increased transcript levels in the p*unh1* strain, as compared to the wild-type (Fig. 6). These increases in transcript level are consistent with the observed pigmentation in culture. Of the three biological replicates of p*unh1* tested, one (p*unh1*-3) produced notably less pigmentation in culture (Fig. S5) and correspondingly had the lowest transcript level of *UMAG_10756* as compared to the other replicates. The data shows the constitutive expression of *unh1* in haploid cells resulted in the formation of spherical cells with increased pigmentation, as well as increased transcript levels of putative pigmentation related genes.

3.5. The identified Ndt80-like DNA-binding domain is required for function

The analysis of the deletion and complementation strains indicated that *unh1* is required for teliospore maturation and meiosis

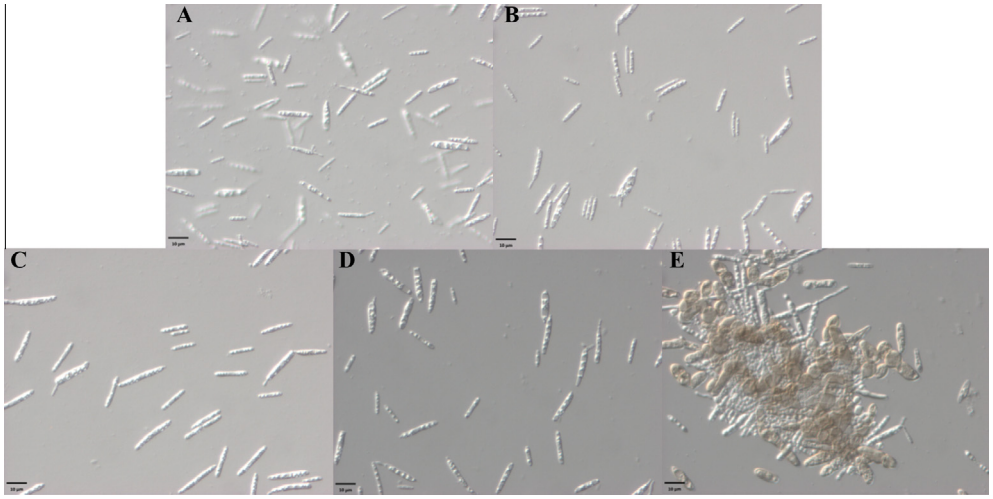

Fig. 5. Growth in PDB with constitutive expression of *unh1* yields altered haploid cell morphology, clumping of cells, and pigmentation. Micrographs of haploid cultures grown in PDB for 7 days (400×). (A) wt, (B) Δ*unh1*, (C) p*unh1*ΔKA, (D) p*unh1*3A, (E) p*unh1*. Scale bar indicates 10 μm.

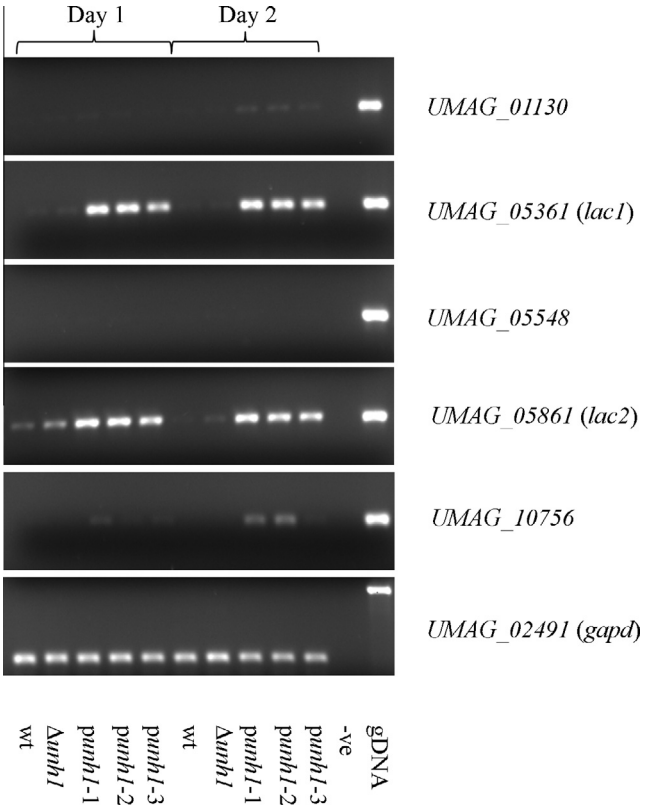

Fig. 6. RT-PCR analysis of genes putatively involved in melanin biosynthesis. RNA was isolated from haploid cultures grown for 24 and 48 h in PDB. Strains are indicated below the gel. 3 biological replicates of p*unh1* were included. Genomic DNA (gDNA) and water (−ve) were used as PCR controls. UMAG identification numbers and names (if applicable) for each gene are given. Transcript levels were compared to those of the housekeeping gene *UMAG_02491* (*gapd*).

completion. *unh1* was originally identified as a putative ortholog to the *S. cerevisiae* gene *NDT80* (Donaldson and Saville, 2008), which encodes a transcription factor that also controls the completion of meiosis. However the sequence similarity was restricted to the Ndt80-like DNA-binding domain (DBD). In the basidiomycetes this domain is toward the c-terminus and the proteins are substantially larger (933aa to 1037aa) than their ascomycete counterparts, which have this DBD toward the N terminus. Unh1 is a 933aa protein containing an Ndt80-like DNA-binding domain (DBD) located between amino acids 641 and 824 (Fig. 7A). The presence of a predicted DBD suggested Unh1, like other Ndt80-like orthologs, was also a transcription factor. Sequencing the *unh1* cDNA revealed that the positions of the spliced introns were different than those predicted in the MUMDB database (Mewes et al., 2008). The cDNA sequence obtained (Fig. S6) led to a re-annotated predicted protein sequence for Unh1 (Fig. S7). The predicted positions of exons, introns and the DBD in *unh1* are shown in Fig. S8. The original predicted annotation for *unh1* in the MUMDB database was 919aa, with the initial 10 amino acids of the DBD being absent from the predicted protein sequence. The re-annotated binding domain was aligned to the Ndt80-like binding domains of other fungal proteins (Fig. 7B) and, based upon these alignments, a phylogenetic tree was constructed that revealed the fungal Ndt80-like proteins examined are split into two distinct groups (Fig. 8). In Fig. 8 the box indicates the group which contains Unh1 and Ndt80. The Unh1 predicted DNA-binding domain (DBD) contains conserved amino acids, known to be involved in the interaction with DNA (Fingerman et al., 2004; Lamoureux and Glover, 2006; Montano et al., 2002a). To determine if this DBD is crucial for the function of Unh1, two binding domain mutant constructs were inserted into the *ip* locus of the Δ*unh1* strain: a DBD deletion mutant, p*unh1*ΔKA; and a DBD mutant in which three conserved arginines (Fingerman et al., 2004) were replaced by alanines, p*unh1*3A (Table 1). These constructs failed to complement the loss of *unh1*. Both p*unh1*ΔKA × Δ*unh1* and p*unh1*3A × Δ*unh1* infections resulted in the formation of teliospores that were smooth and pale in color (Fig. 4D and E), similar to Δ*unh1* × Δ*unh1* infections (Fig. 4B), in distinct contrast to the appearance of the wt × wt and Δ*unh1* × wt teliospores (Fig. 4A). These DBD mutants also failed to complement the meiosis defect in Δ*unh1* strains, with over 90% of the teliospores from each cross germinating to produce colonies that grew on both types of selection (Table 2). Further, the binding domain mutant strains did not produce the pigmentation phenotype in PDB. While the p*unh1* strain resulted in the irregular growth of cells and pigmentation, the p*unh1*ΔKA and p*unh1*3A strains, retained the appearance of the wt and Δ*unh1* cultures (Fig. 5C and D). This indicated that these two complementation strains contain a form of Unh1 that is either non-functional, or severely limited in function.

3.6. Unh1 alters the transcript levels of putative downstream target genes

The requirement of the DNA-binding domain for function indicates that Unh1, like other members of the Ndt80 family, is a DNA-binding protein. The fact that three key amino acids, known to be involved with DNA interaction (Fingerman et al., 2004; Lamoureux and Glover, 2006; Montano et al., 2002a), are required for *U. maydis* Unh1 to function, suggests that Unh1 is a transcription factor that recognizes a sequence similar to other Ndt80-like proteins. Based on this, possible Unh1 downstream target genes were identified by searching the upstream region of *U. maydis* genes for variants of the MSE, the well characterized Ndt80-like protein DNA binding motif, using DNA Pattern Find (Stothard, 2000). 89 genes with predicted upstream MSEs were screened by RT-PCR, using RNA isolated from dormant teliospores of wild-type and Δ*unh1* × Δ*unh1* strains. The results suggested that transcript levels for 43 of these genes were altered in Δ*unh1* × Δ*unh1* teliospores relative to wild-type. Of these, 12 genes were selected for further screening using RT-qPCR (Fig. 9), which allowed the confirmation of two genes with increased transcript levels, as well as three with decreased transcript levels (Fig. 10), in the Δ*unh1* × Δ*unh1* teliospores relative to the wild-type teliospores. With these target genes identified, the upstream regions were screened for the presence of conserved sequence elements using MEME (Bailey and Elkan, 1994). Two motifs were identified that bore similarity to the known MSE from *S. cerevisiae* (Fig. 11). Motif A was found upstream of two of the three putative target genes that had decreased transcript levels in Δ*unh1* × Δ*unh1* teliospores, while motif B was present upstream of all five predicted Unh1 target genes. These motifs were compared to known motifs in the JASPAR database using TOMTOM (Gupta et al., 2007), which identified the similarity to the Ndt80 MSE (Fig. 11). These identified motifs may be involved in the regulation of Unh1 target genes.

4. Discussion

4.1. Unh1, an Ndt80-like DNA-binding protein

U. maydis Unh1 belongs to the Ndt80-like DNA-binding family of proteins. Katz et al. (2013) reviewed the occurrences of this class of proteins in fungi and reported they were common in ascomycota, chytridiomycota and zygomycota, but rare among the

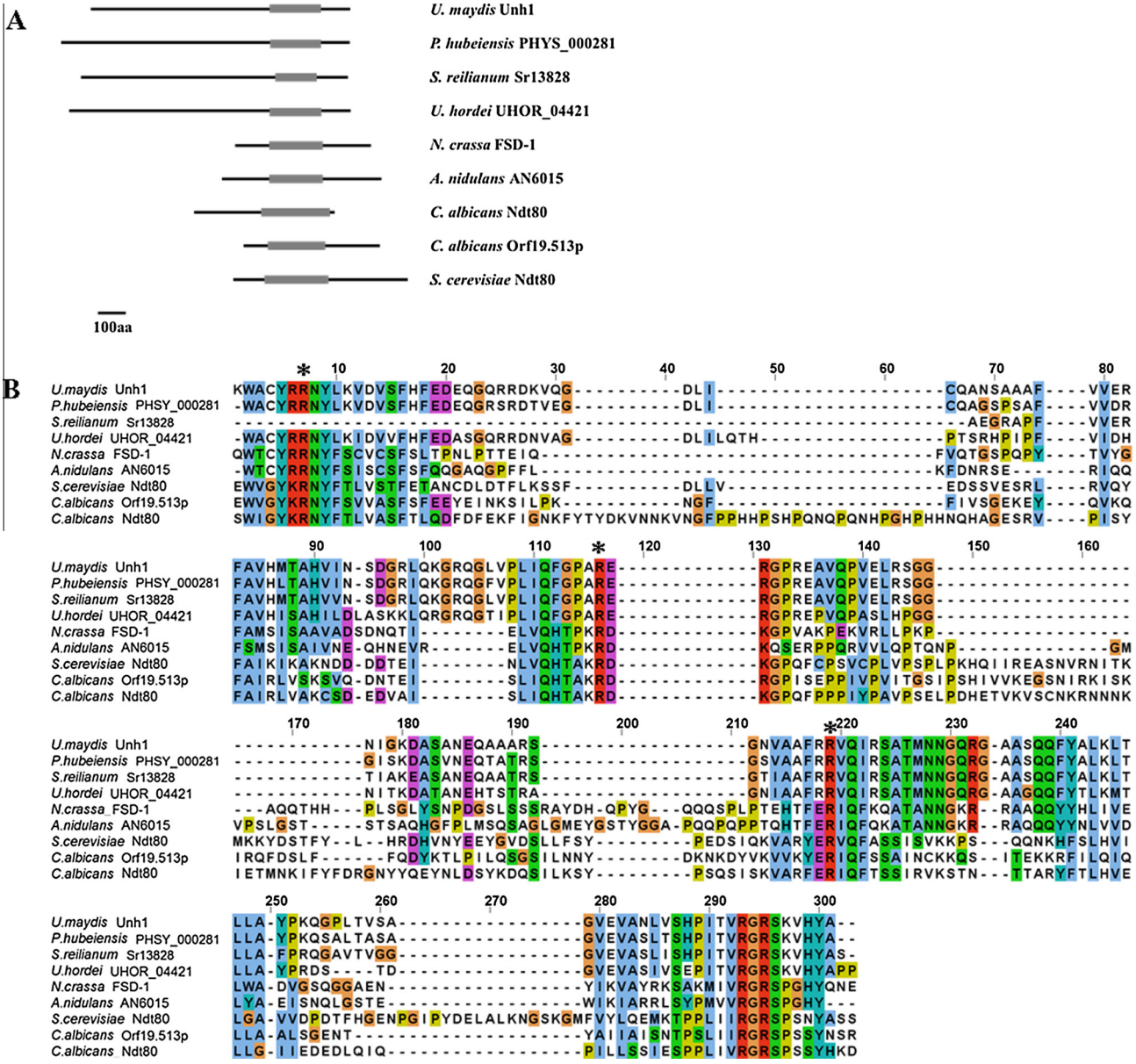

Fig. 7. Alignment of Ndt80 DNA-binding domain proteins. (A) Location of the Ndt80 DNA-binding domain in Unh1 and putative orthologs in the same clade. The domain, identified by protein blast (Altschul et al., 1990), is indicated in grey. Proteins and domains are to scale, 100aa length is indicated by the scale bar. (B) Sequence alignment of the DNA-binding domain of Unh1 and putative orthologs. Binding domains were identified by using protein blast (Altschul et al., 1990) and aligned using MAFFT (Goujon et al., 2010; Katoh and Toh, 2008; McWilliam et al., 2013). Visualized using JalView (Waterhouse et al., 2009), with Clustal X color scheme. Stars indicate the position of the conserved amino acids: R647, R720 and R761. (For interpretation of the references to color in this figure legend, the reader is referred to the web version of this article.)

basidiomycota, being found in the ustilaginomycotina but not the pucciniomycotina or agaricomycotina. Unh1 is the first member of this family characterized in the basidiomycetes. The similarity between Unh1 and other members of the Ndt80-like DNA-binding family lies only in the region of the DNA-binding domain, a trait common among Ndt80 homologs (Hutchison and Glass, 2010; Wang et al., 2006). The Bayesian phylogenetic tree, based on aligning these DNA-binding domains (Fig. 7B), revealed two clades (Fig. 8), one containing proteins involved in sexual reproduction and the other, proteins involved in nutrient sensing that triggers distinct responses (Chu and Herskowitz, 1998; Dementhon et al., 2006; Hutchison and Glass, 2010; Katz et al., 2006, 2013; Xiang and Glass, 2002). With the exception of the non-sexual *Candida albicans*, when more than one Ndt80-like DNA-binding protein is present, those involved in sexual reproduction and those involved in other responses to environmental conditions, branch separately. This division has been previously observed (Hutchison and Glass, 2010) and indicates that Ndt80-like proteins in fungi retain the ancestral nutrient sensing common to the p53 super-family (Katz et al., 2013), but only certain family members link this sensing to reproduction and even fewer link it to meiosis. In *S. cerevisiae* Ndt80 is a transcription factor, involved in the completion of meiosis (Chu et al., 1998; Chu and Herskowitz, 1998; Hepworth et al., 1998) and Unh1 is linked to meiosis in *U. maydis*. This suggests that nutrient sensing through Ndt80 and Unh1 is linked to meiosis.

The DNA-binding domain (DBD) of Unh1 is crucial to its function, and it shares notable similarity to that of Ndt80, which is required for the full expression of middle meiosis genes in *S. cerevisiae* (Chu et al., 1998; Chu and Herskowitz, 1998; Hepworth et al., 1998). The Ndt80 DBD binds to the middle sporulation element (MSE), located in the promoter region of many target genes (Chu and Herskowitz, 1998). *U. maydis* strains were

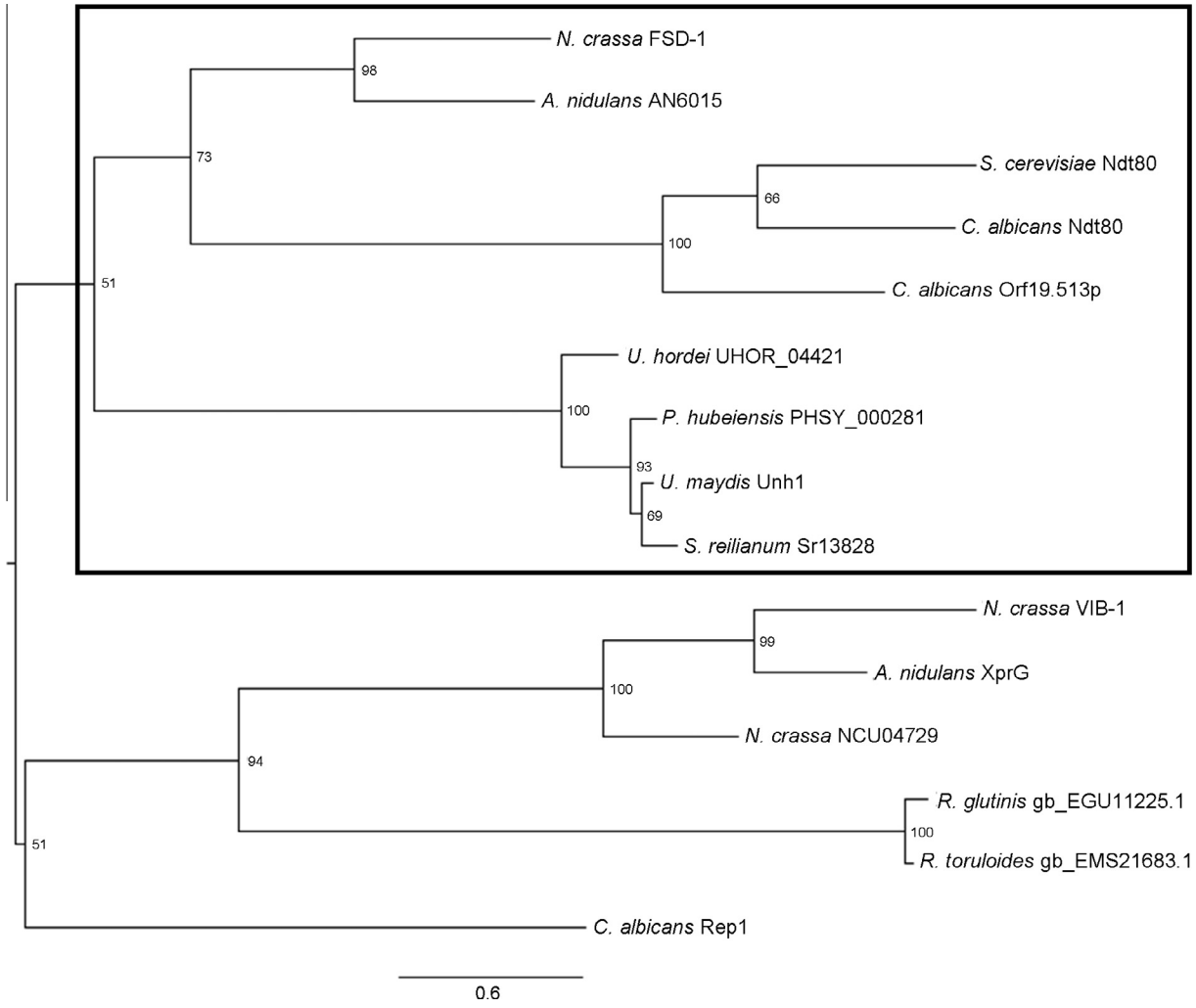

Fig. 8. Bayesian consensus tree demonstrating a phylogeny of Unh1 orthologs. This tree was created using MRBAYES 3.2 (Huelsenbeck and Ronquist, 2001; Ronquist and Huelsenbeck, 2003), using an LG + G amino acid substitution model. The tree is rooted at the mid-point and the posterior probability for each split is indicated. The scale bar indicates expected substitutions per site. The tree was visualized with FigTree (http://tree.bio.ed.ac.uk/software/figtree/). The name of the protein or the accession number is indicated. The box delineates the clade containing Unh1.

created wherein either the entire Unh1 DBD was deleted or Unh1 R647, R720 and R761 were mutated to alanines. These conserved arginines are involved in crucial base-specific interactions with the MSE in *S. cerevisiae* (Fingerman et al., 2004; Lamoureux et al., 2002; Montano et al., 2002a, 2002b). Both mutant *unh1* strains were phenotypically indistinguishable from Δ*unh1* strains, indicating that the DNA binding domain, and specifically the three conserved arginines, may be necessary for Unh1 function. It is also possible that these mutations destabilize Unh1. However, the structural and functional similarity to Ndt80 suggests that Unh1 is a DNA-binding protein, and likely a transcription factor.

4.2. Unh1 alters transcript levels of genes in U. maydis

The DBD conservation between Unh1 and Ndt80 suggested that Unh1 may have a DNA target similar to the MSE. In *C. albicans*, CaNdt80 also binds MSEs (Sellam et al., 2010). The consensus sequence for the Ndt80 MSE is gNCRCAAAW (Chu and Herskowitz, 1998). 89 *U. maydis* genes with either canonical or less stringent possible MSE (GNCRCNNNN), were screened by RT-PCR in wild-type and Δ*unh1* × Δ*unh1* teliospores. 43 of these genes had transcript levels that differed from the wild-type. The transcript levels of 12 of the 43 genes was assessed by RT-qPCR (Fig. 9), which confirmed two genes with increased transcript levels and three with decreased transcript levels in the Δ*unh1* × Δ*unh1* teliospores, relative to wild-type (Fig. 10). The increased or decreased transcript levels of target genes indicated that either Unh1 can act as both an activator and repressor, or that Unh1 indirectly altered transcript levels of some genes. CaNdt80 functions as both a positive and negative regulator of transcription, a trait common to members of the p53 family of transcription factors, to which the Ndt80-like DNA-binding family belongs (Sellam et al., 2010). Of the five genes with varied transcript levels, *UMAG_05664* was identified as a possible ortholog to the *S. cerevisiae* gene *DIT2* (Donaldson and Saville, 2008), which is involved in ascospore wall formation and is a putative target of Ndt80 (Bogengruber et al., 1998; Briza et al., 1994). Searching the upstream regions of the 5 potential Unh1 target genes for conserved motifs revealed two with similarity to the MSE in *S. cerevisiae* (Fig. 11). In motif A there was strong similarity to the MSE at positions 9, 11 and 12, where R111, R177, and R254 of Ndt80 have been shown to interact. Further research into the *in vitro* and *in vivo* function of this motif may lead to the refinement of the sequence to which Unh1 binds in *U. maydis*.

It was initially of concern that only a few of the genes with an MSE-like motif had altered transcript levels in the absence of

FB1xFB2	ΔxΔ	gDNA	-ve	Gene	Description	MSE
				UMAG_00983	conserved hypothetical protein	1
				UMAG_06485	putative protein	0
				UMAG_10186	putative protein	1
				UMAG_04827	probable PPZ2 - protein ser/thr phosphatase of the PP-1 family	1
				UMAG_05664	related to cytochrome P450	1
				UMAG_11505	putative protein	0
				UMAG_00196	probable FUN34 - transmembrane protein involved in ammonia production	1
				UMAG_02713	pheromone response factor Prf1	1
				UMAG_10350	putative protein	1
				UMAG_04543	related to protein kinase Lkh1	1
				UMAG_12194	conserved hypothetical protein	1
				UMAG_11308	histone deacetylase	1

Fig. 9. RT-PCR analysis of putative Unh1 target genes. RNA was isolated from dormant teliospores harvested from corn cob infections. FB1 × FB2 indicates a wild-type cross, ΔxΔ indicates a Δ*unh1* × Δ*unh1* cross. Genomic DNA (gDNA) and water (−ve) were used as PCR controls. UMAG identification numbers and predicted functions, as presented on MUMDB (Mewes et al., 2008), are provided for each gene, along with the number of canonical middle sporulation elements (MSEs) that were identified in the upstream regions.

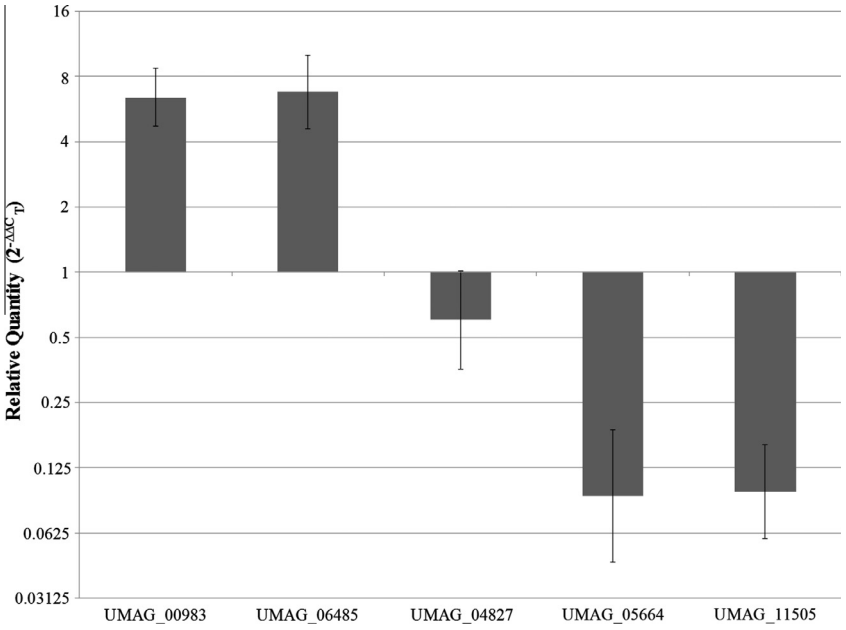

Fig. 10. Deletion of *unh1* alters the transcript level of putative downstream target genes. Relative quantities of target gene transcripts in Δ*unh1* × Δ*unh1* teliospores relative to wild-type teliospores. RT-qPCR determinations of relative transcript levels were calculated using the comparative C_T ($2_T^{-\Delta\Delta C}$) method, with *UMAG_00175* acting as the endogenous control and wild-type teliospores as the calibrator. Bars indicate RQ maximum and RQ minimum values (95% confidence interval, n = 2).

unh1; however, in *S. cerevisiae* there is an MSE upstream of 1/3 of all genes, yet only approximately 200 have transcript levels altered by ectopic expression of Ndt80 (Chu et al., 1998). Furthermore, only ~62% of genes induced by Ndt80 contained an MSE (Chu et al., 1998) and in *C. albicans CaNDT80* deletion did not always affect expression of genes that were shown to be bound by CaNdt80. This was interpreted as an indicator of cell type specific control, or of other proteins compensating for CaNdt80 loss (Sellam et al., 2010). So it is possible that Unh1 may influence expression of genes with MSE-like motif even though the

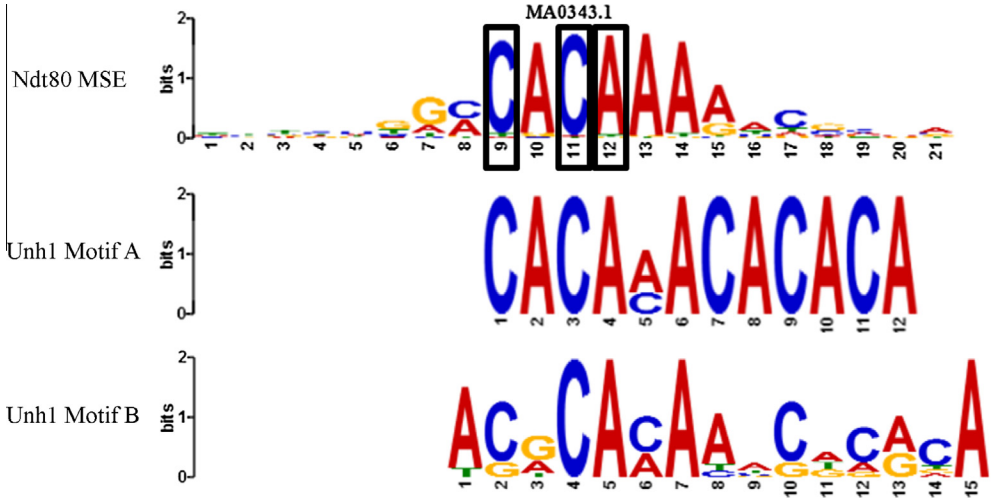

Fig. 11. Motifs located upstream of putative Unh1 target genes. Motif A was present upstream of 2 of the 3 predicted target genes with decreased transcript levels in Δ*unh1* teliospores. Motif B was present upstream of all 5 predicted Unh1 target genes. Black boxes indicate bases involved in protein binding with R111, R177, and R254 of Ndt80. Motifs were identified using MEME (Bailey and Elkan, 1994) and compared to known motifs in the JASPAR database using TOMTOM (Gupta et al., 2007).

experiments carried out did not show an alteration in transcript level or that only a few of the genes with MSE-like motif are directly controlled by Unh1.

4.3. Unh1 is required for teliospore maturation and pigmentation

The development of teliospores in Δ*unh1* × Δ*unh1* and wild-type infections were compared to the previous morphological characterization of teliospore formation *in planta.* Microscopic examination of wild-type strains in the current study was consistent with the developmental progression previously described (Banuett and Herskowitz, 1996), though teliospore maturation occurred slightly earlier, possibly due to differences in corn host variety. However, the Δ*unh1* × Δ*unh1* infections progressed normally only up until the initiation of teliospore development, at which point there was a delay, with immature teliospores not appearing until 11 dpi, 2 days later than in the wild-type. Δ*unh1* × Δ*unh1* teliospores were also much less abundant than in the wild-type. Mature, pigmented teliospores, which appeared at 12 dpi in wild-type, never developed in the Δ*unh1* × Δ*unh1* infections (Fig. 2). The deletion of *unh1*, therefore, causes a defect after teliospore formation initiates, but before the deposition of the mature cell wall.

The cell wall in *U. maydis* teliospores is deposited in three layers: the sheath, the exosporium and the endosporium (Piepenbring et al., 1998a; Ramberg and McLaughlin, 1980). The teliospore initials embedded in the mucilaginous matrix first develop the sheath, a hyaline envelope that distinguishes it from the matrix. Next, ornamentation, like the echinulation in *U. maydis*, forms on the plasma membrane under the sheath (Piepenbring et al., 1998b). The exosporium forms after the ornamentation. This is the continuous layer that develops underneath the sheath and contains the ornamentation and dark melanin deposits (Bell and Wheeler, 1986; Piepenbring et al., 1998a; Ramberg and McLaughlin, 1980). Finally, the innermost layer is formed, the light-colored endosporium (Piepenbring et al., 1998a). In the Unh1 mutants, teliospore formation was abnormal, but immature spores, separate from the mucilaginous matrix, were present, indicating the formation of the sheath. However, the ornamentation did not appear to develop, as the mutant teliospores were smooth in appearance. The unusual shape of the mutant teliospores, which were often oblong or bent instead of spherical, and the pale color, indicated that the thick, melanized exosporium was not properly formed. It was unclear whether the endosporium formed, however the mutant *unh1* teliospores were able to germinate and form a promycelium, and the promycelial wall is believed to be derived from the endosporium layer, which may also provide nutrients for germination (Piepenbring et al., 1998b; Ramberg and McLaughlin, 1980). As Δ*unh1* × Δ*unh1* teliospores germinate viably (Fig. 3C and D), this could indicate that the endosporium did form, despite the abnormal exosporium. Finally, possibly due to the defects in teliospore maturation, the mucilaginous matrix did not appear to dissipate in the mutants. Normally, the matrix disappears as the teliospores mature, resulting in the dry, dusty appearance common to the matured teliospores in *U. maydis* (Piepenbring et al., 1998a). The teliospores from the Δ*unh1* × Δ*unh1* infections often appeared to remain embedded in the matrix, and dusty teliospore masses never formed. Hence, teliospore maturation and pigmentation are affected by Unh1. Based on the defective phenotype induced by *unh1* deletion, it is likely that Unh1 functions after the initiation of teliospore formation, during maturation and ornamentation of the teliospores.

A role for Unh1 in controlling teliospore pigmentation was supported by the phenotype of the p*unh1* strain. This haploid strain constitutively expresses *unh1* and has an elevated *unh1* transcript level. In nutrient limited medium, cells became rounded and pigmented, in contrast to the normal cigar-shape and light-coloration of haploids (Fig. 5). This impact on pigmentation is consistent with the phenotype that resulted from deletion of *unh1*, which led to the absence of pigmentation in the normally dark teliospores. Combined, these results suggested that environmental and/or nutritional signals influence *U. maydis* teliospore maturation and pigmentation *in planta.* Nutrient sensing is a conserved feature in Ndt80-like proteins (Katz et al., 2006, 2013) and specific Ndt80 homologs are involved in pigmentation and cell wall formation. Ndt80 regulates ascospore formation (Chu et al., 1998; Chu and Herskowitz, 1998) and *Aspergillus nidulans xprG* and *Neurospora crassa fsd-1* are both involved in spore pigmentation (Hutchison and Glass, 2010; Katz et al., 2013). Unh1 appears to control melanin biosynthesis and cell wall development, indicating that this may be an ancestral role. The increased transcript levels of two predicted tyrosinases, and the two predicted laccases present in the *U. maydis* genome (*lac1* and *lac2*) in the p*unh1*, when grown in pigment inducing conditions support this role for Unh1. Additionally, one specific strain of *punh1* produced less pigment than the others (Fig. S5), and correspondingly had lower transcript

levels of one of the tyrosinases (*UMAG_10756*, Fig. 6). This reinforces the link between pigmentation and these genes.

Tyrosinases and laccases are enzymes often involved in fungal melanin biosynthesis (Bell and Wheeler, 1986; Jolivet et al., 1998). *lac1* and *lac2*, were also highly expressed in *U. maydis ust1* deletion strains, which produced abnormal pigmentation in axenic culture, and Δ*lac1* strains were shown to result in decreased pigmentation (Islamovic et al., 2015). Previous studies supported catechol based production of melanin (Piatelli et al., 1963, 1965; Bell and Wheeler, 1986; Wheeler, 1983) and, separately, DHN based biosynthesis (Islamovic et al., 2015). Characterization of the 4 genes identified here as involved in pigment production may assist in elucidating the melanin biosynthetic pathway in *U. maydis*.

4.4. Unh1 plays a key role in meiosis in U. maydis

The completion of meiosis was assessed by germinating teliospores and determining the segregation of antimycotic resistance in the progeny. To confirm that these results were due to the failure of meiotic segregation during germination, and not due to contamination with diploid cells potentially isolated from tumors, these results were confirmed by treating isolated teliospores with copper sulfate before germination for 3 h. This treatment was sufficient to kill haploid *U. maydis* cells, but not teliospores. Δ*unh1* × Δ*unh1*, with their immature cell walls, were more sensitive to $CuSO_4$ treatment, with longer treatments negatively impacting viability. Teliospores resulting from Δ*unh1* × wt and p*unh1* × Δ*unh1* infections displayed segregation of resistance, indicating that meiosis completed normally and that the mutant phenotype is recessive. χ^2 tests showed that the observed resistance phenotypes differed from that expected for random segregation in the teliospores obtained from p*unh1* × Δ*unh1* infections. This may be a consequence of scoring segregation of inserted antimycotic genes and the fact that *carbR* is located at two separate loci. However, it is clear that meiosis was restored in the complemented strains since segregation of resistance to antimycotics did occur. In teliospores isolated from the Δ*unh1* × Δ*unh1*, p*unh1*ΔKA × Δ*unh1* and p*unh1*3A × Δ*unh1* infections, segregation of resistance is significantly impaired (χ^2, $p > 0.05$). Additionally, progeny from Δ*unh1* × Δ*unh1* teliospore germinations were able to infect corn seedlings without a mating partner and cause disease symptoms consistent with solopathogenic diploid infections (Kruskal-Wallis test and Dunn multiple comparison, $p > 0.05$). The observed reduction in virulence of diploid infections relative to dikaryon infections is consistent with previous studies (Babu et al., 2005). Together these results indicated that meiosis was highly deficient when *unh1* is deleted, or when its DBD is deleted or mutated, confirming that Unh1 is required for meiosis completion and that the DBD of Unh1 is crucial for this function.

Unh1 teliospores are highly deficient in meiosis completion, but are capable of germination, indicating a return to mitotic growth after teliospore formation. This has been observed in *S. cerevisiae*, where in the absence of *NDT80*, meiosis is not completed, arresting at the pachytene checkpoint, before the first meiotic divisions (Xu et al., 1995). These arrested cells were fully capable of returning to mitotic growth, under suitable conditions (Xu et al., 1995). The pachytene checkpoint, the point from which the cell can return to mitotic growth before reductional divisions, controls both the expression and post-translational activity of Ndt80, resulting in arrest if the checkpoint is not cleared (Hepworth et al., 1998; Pak and Segall, 2002; Shuster and Byers, 1989; Tung et al., 2000). Ndt80 is thus essential to the commitment to, and completion of, meiosis. In *U. maydis*, meiosis begins *in planta* (Donaldson and Saville, 2008; Saville et al., 2012) then arrests after recombination, but before meiotic divisions, likely in late prophase I (Kojic et al., 2013). Teliospores germinate in late prophase I (O'Donnell and McLaughlin, 1984) and meiosis is completed during germination. This indicates that germination signals the exit from the pachytene checkpoint and the entry into meiotic divisions (Kojic et al., 2013). The phenotype of the Δ*unh1* × Δ*unh1* teliospores is consistent with Unh1 being required for release from the pachytene checkpoint in *U. maydis* since, without it, meiotic divisions do not occur and most teliospores germinate without completing meiosis and grow mitotically as diploids.

If Unh1 is involved in pachytene checkpoint control, as Ndt80 is in *S. cerevisiae*, it would be expected that the arrest in the *unh1* mutants also occurred around the time the teliospore entered dormancy, which is believed to be at the pachytene checkpoint. This is supported by the observation that deletion of *spo11*, involved in double strand break formation, has a deleterious effect on pathogenesis in *U. maydis*, while deletion of genes that affect meiotic recombination processes downstream of Spo11, like *brh2* and *rad51*, have not been shown to impact virulence (Kojic et al., 2013). As Δ*unh1* does not alter pathogenesis, but does influence teliospore development and meiotic completion, this would likely place it downstream of the initiation of meiosis and of Spo11, but prior to meiotic divisions. This timing was confirmed by investigations that showed *unh1* is a target of Ros1 (Tollot et al., 2016) and is consistent with Unh1 being involved in exit from the pachytene checkpoint.

4.5. Comparing Unh1 to other U. maydis genes involved in teliospore formation

In *U. maydis*, Unh1 defects cause alterations in pigmentation, teliospore maturation, and meiosis completion. The Ndt80-like DBD was required for Unh1 function. It was shown that environmental conditions, and possibly nutrition, could impact the function of Unh1 *in vivo*. This may indicate that Unh1 responds to environmental signals, likely from the plant, and that these signals play a role in the development of teliospores, and the commitment to meiosis. How this signal is transmitted to Unh1 will be crucial for understanding how the meiotic process is regulated in the plant.

Several characterized genes, including *cru1*, *ust1*, and *hgl1*, influence teliospore formation and pigmentation, resembling the phenotype observed in *unh1* mutants. *cru1* mutants produced small numbers of non-viable teliospores that were irregular in shape and pigmentation. Nutrient content of the medium altered expression of *cru1* (Castillo-Lluva et al., 2004). *ust1* is required for mating and gall formation *in planta* and *ust1* null mutants grow in PDB as both filaments and rounded, pigmented cells (García-Pedrajas et al., 2010). Furthermore, Ust1 appears to regulate genes involved in melanin biosynthesis and teliosporogenesis (Islamovic et al., 2015). *hgl1* is also involved in filamentous growth and teliosporogenesis, and *hgl1* deletion mutants develop abnormal pigmentation when grown on PD medium (Dürrenberger et al., 2001). This indicates that *unh1* is part of a growing group of genes that link teliospore formation to nutritional signaling, with PD and other less nutrient rich media triggering the formation of teliospore like structures, or the expression of genes involved in teliospore formation, in mutant strains. However, the effect of *unh1* deletion is limited to teliospore maturation, while *cru1*, *ust1* and *hgl1* all impact pathogenesis as well (Castillo-Lluva et al., 2004; Dürrenberger et al., 2001; García-Pedrajas et al., 2010). This suggests that these genes may function upstream of *unh1* and may relay a signal to Unh1 to influence its role in teliospore formation and pigmentation.

5. Conclusion

Unh1 plays a crucial role in the sexual development of *U. maydis*. Functional analyses revealed that it affects the successful completion of meiosis, teliospore wall formation and the melanin biosynthesis pathway. The DBD is crucial to the function of Unh1, and it shares conservation with other members of the Ndt80-like DNA-binding proteins. However, lack of conservation outside of the DBD suggests that Unh1 may respond to signals that are unique to *U. maydis*, or to development in the plant. In haploid cells that constitutively express Unh1, its activity and phenotype is modulated by nutritional status, suggesting that Unh1 may be responding to nutritional state during growth in the plant. As such, the study of Unh1 opens crucial avenues of study to better elucidate the still poorly characterized processes of teliospore maturation and pigmentation in *U. maydis*. It may also provide a link between teliospore development, *in planta* development, and nutritional signaling. These processes are critical to pathogenesis in the smuts and rusts, so this first characterization of an Ndt80-like DNA-binding protein in the basidiomycete fungi provides a basis for investigating signaling and pathogenic development in the less tractable basidiomycete biotrophic fungi.

Acknowledgements

We would like to acknowledge Erin Morrison, Michael Donaldson, Vythegi Srithayakumar, Lauren Ostrowski and Kristi Goulet for critical reading of this manuscript. Also, Amanda Seto, for technical assistance and Amanda Ker for data collection. Funding for this project was awarded through the Natural Sciences and Engineering Research Council (NSERC) of Canada (BJS), NSERC scholarships, (CED, HYKC) and Ontario Graduate Scholarships (CED).

Appendix A. Supplementary material

Supplementary data associated with this article can be found, in the online version, at http://dx.doi.org/10.1016/j.fgb.2016.07.006.

References

Altschul, S.F. et al., 1990. Basic local alignment search tool. J. Mol. Biol. 215, 403–410.
Babu, M.R. et al., 2005. Differential gene expression in filamentous cells of *Ustilago maydis*. Curr. Genet. 47, 316–333.
Bailey, T.L., Elkan, C., 1994. Fitting a mixture model by expectation maximization to discover motifs in biopolymers. Proceedings of the Second International Conference on Intelligent Systems for Molecular Biology, vol. 2, pp. 28–36.
Bailis, J.M., Roeder, G.S., 2000. Pachytene exit controlled by reversal of Mek1-dependent phosphorylation. Cell 101, 211–221.
Banuett, F., 1995. Genetics of *Ustilago maydis*, a fungal pathogen that induces tumors in maize. Annu. Rev. Genet. 29, 179–208.
Banuett, F., Herskowitz, I., 1989. Different a alleles are necessary for maintenance of filamentous growth but not for meiosis. Proc. Natl. Acad. Sci. USA 86, 5878–5882.
Banuett, F., Herskowitz, I., 1996. Discrete developmental stages during teliospore formation in the corn smut fungus, *Ustilago maydis*. Development 122, 2965–2976.
Basse, C.W. et al., 2000. Characterization of a *Ustilago maydis* gene specifically induced during the biotrophic phase: evidence for negative as well as positive regulation. Mol. Cell. Biol. 20, 329–339.
Bell, A.A., Wheeler, M.H., 1986. Biosynthesis and functions of fungal melanins. Annu. Rev. Phytopathol. 24, 411–451.
Bogengruber, E. et al., 1998. Sporulation-specific expression of the yeast DIT1/DIT2 promoter is controlled by a newly identified repressor element and the short form of Rim101p. Eur. J. Biochem. 258, 430–436.
Brachmann, A. et al., 2004. A reverse genetic approach for generating gene replacement mutants in *Ustilago maydis*. Mol. Genet. Genomics 272, 216–226.
Brefort, T. et al., 2009. *Ustilago maydis* as a pathogen. Annu. Rev. Phytopathol. 47, 423–445.
Briza, P. et al., 1994. The sporulation-specific enzymes encoded by the DIT1 and DIT2 genes catalyze a two-step reaction leading to a soluble LL-dityrosine-containing precursor of the yeast spore wall. Proc. Natl. Acad. Sci. USA 91, 4524–4528.
Bryne, J.C. et al., 2008. JASPAR, the open access database of transcription factor-binding profiles: new content and tools in the 2008 update. Nucleic Acids Res. 36, D102–D106.
Castillo-Lluva, S. et al., 2004. A member of the Fizzy-related family of APC activators is regulated by cAMP and is required at different stages of plant infection by *Ustilago maydis*. J. Cell Sci. 117, 4143–4156.
Christensen, J.J., 1931. Studies on the genetics of *Ustilago maydis*. Phytopathol. Z. 4, 129–188.
Chu, S. et al., 1998. The transcriptional program of sporulation in budding yeast. Science 282, 699–705.
Chu, S., Herskowitz, I., 1998. Gametogenesis in yeast is regulated by a transcriptional cascade dependent on Ndt80. Mol. Cell 1, 685–696.
Darriba, D. et al., 2011. ProtTest 3: fast selection of best-fit models of protein evolution. Bioinformatics 27, 1164–1165.
Dementhon, K. et al., 2006. VIB-1 is required for expression of genes necessary for programmed cell death in *Neurospora crassa*. Eukaryot. Cell 5, 2161–2173.
Donaldson, M.E., Saville, B.J., 2008. Bioinformatic identification of *Ustilago maydis* meiosis genes. Fungal Genet. Biol. 45 (Suppl. 1), S47–S53.
Dürrenberger, F. et al., 2001. The hgl1 gene is required for dimorphism and teliospore formation in the fungal pathogen *Ustilago maydis*. Mol. Microbiol. 41, 337–348.
Fingerman, I.M. et al., 2004. Characterization of critical interactions between Ndt80 and MSE DNA defining a novel family of Ig-fold transcription factors. Nucleic Acids Res. 32, 2947–2956.
Finn, R.D. et al., 2014. Pfam: the protein families database. Nucleic Acids Res. 42, D222–D230.
García-Pedrajas, M.D. et al., 2010. Regulation of *Ustilago maydis* dimorphism, sporulation, and pathogenic development by a transcription factor with a highly conserved APSES domain. Mol. Plant Microbe Interact. 23, 211–222.
Gold, S.E. et al., 1997. The *Ustilago maydis* regulatory subunit of a cAMP-dependent protein kinase is required for gall formation in maize. Plant Cell 9, 1585–1594.
Goujon, M. et al., 2010. A new bioinformatics analysis tools framework at EMBL-EBI. Nucleic Acids Res. 38, W695–W699.
Guindon, S., Gascuel, O., 2003. A simple, fast, and accurate algorithm to estimate large phylogenies by maximum likelihood. Syst. Biol. 52, 696–704.
Gupta, S. et al., 2007. Quantifying similarity between motifs. Genome Biol. 8, R24.
Hepworth, S.R. et al., 1998. NDT80 and the meiotic recombination checkpoint regulate expression of middle sporulation-specific genes in *Saccharomyces cerevisiae*. Mol. Cell. Biol. 18, 5750–5761.
Holliday, R., 1961. Induced mitotic crossing-over in *Ustilago maydis*. Genet. Res. 2, 231–248.
Holliday, R., 1974. *Ustilago maydis*. In: King, R.C. (Ed.), Handbook of Genetics. Plenum Press, New York, pp. 575–595.
Huelsenbeck, J.P., Ronquist, F., 2001. MRBAYES: Bayesian inference of phylogeny. Bioinformatics 17, 754–755.
Hutchison, E.A., Glass, N.L., 2010. Meiotic regulators Ndt80 and Ime2 have different roles in *Saccharomyces* and *Neurospora*. Genetics 185, 1271–1282.
Islamovic, E. et al., 2015. Transcriptome analysis of a *Ustilago maydis* ust1 deletion mutant uncovers involvement of laccase and polyketide synthase genes in spore development. Mol. Plant Microbe Interact. 28, 42–54.
Jolivet, S. et al., 1998. *Agaricus bisporus* browning: a review. Mycol. Res. 102, 1459–1483.
Kahmann, R., Kämper, J., 2004. *Ustilago maydis*: how its biology relates to pathogenic development. New Phytol. 164, 31–42.
Kämper, J., 2004. A PCR-based system for highly efficient generation of gene replacement mutants in *Ustilago maydis*. Mol. Genet. Genomics 271, 103–110.
Kämper, J. et al., 2006. Insights from the genome of the biotrophic fungal plant pathogen *Ustilago maydis*. Nature 444, 97–101.
Katoh, K., Toh, H., 2008. Recent developments in the MAFFT multiple sequence alignment program. Brief. Bioinf. 9, 286–298.
Katz, M.E. et al., 2013. A p53-like transcription factor similar to Ndt80 controls the response to nutrient stress in the filamentous fungus, *Aspergillus nidulans*. F1000Research 2.
Katz, M.E. et al., 2006. The *Aspergillus nidulans* xprG (phoG) gene encodes a putative transcriptional activator involved in the response to nutrient limitation. Fungal Genet. Biol. 43, 190–199.
Kojic, M. et al., 2002. BRCA2 homolog required for proficiency in DNA repair, recombination, and genome stability in *Ustilago maydis*. Mol. Cell 10, 683–691.
Kojic, M. et al., 2013. Initiation of meiotic recombination in *Ustilago maydis*. Genetics 195, 1231–1240.
Lamoureux, J.S., Glover, J.N., 2006. Principles of protein-DNA recognition revealed in the structural analysis of Ndt80-MSE DNA complexes. Structure 14, 555–565.
Lamoureux, J.S. et al., 2002. Structure of the sporulation-specific transcription factor Ndt80 bound to DNA. EMBO J. 21, 5721–5732.
Martinez-Espinoza, A.D. et al., 2002. The Ustilaginales as plant pests and model systems. Fungal Genet. Biol. 35, 1–20.
McWilliam, H. et al., 2013. Analysis tool web services from the EMBL-EBI. Nucleic Acids Res. 41, W597–W600.
Mewes, H.W. et al., 2008. MIPS: analysis and annotation of genome information in 2007. Nucleic Acids Res. 36, D196–D201.
Montano, S.P. et al., 2002a. Crystal structure of the DNA-binding domain from Ndt80, a transcriptional activator required for meiosis in yeast. Proc. Natl. Acad. Sci. USA 99, 14041–14046.

Montano, S.P. et al., 2002b. Crystallographic studies of a novel DNA-binding domain from the yeast transcriptional activator Ndt80. Acta Crystallogr., D: Biol. Crystallogr. 58, 2127–2130.
Morrison, E.N. et al., 2012. Identification and analysis of genes expressed in the *Ustilago maydis* dikaryon: uncovering a novel class of pathogenesis genes. Can. J. Plant Pathol. 34, 417–435.
O'Donnell, K., McLaughlin, D., 1984. Ultrastructure of meiosis in *Ustilago maydis*. Mycologia, 468–485.
Pak, J., Segall, J., 2002. Role of Ndt80, Sum1, and Swe1 as targets of the meiotic recombination checkpoint that control exit from pachytene and spore formation in *Saccharomyces cerevisiae*. Mol. Cell. Biol. 22, 6430–6440.
Piatelli, M. et al., 1963. *Ustilago* melanin, a naturally occuring catechol melanin. Tetrahedron Lett. 15, 997–998.
Piatelli, M. et al., 1965. The structure of melanins and melanogenesis-V: Ustilagomelanin. Tetrahedron 21, 3229–3236.
Piepenbring, M. et al., 1998a. Teliospores of smut fungi – general aspects of teliospore walls and sporogenesis. Protoplasma 204, 155–169.
Piepenbring, M. et al., 1998b. Teliospores of smut fungi – teliospore walls and the development of ornamentation studied by electron microscopy. Protoplasma 204, 170–201.
Ramberg, J.E., McLaughlin, D.J., 1980. Ultrastructural study of promycelial development and basidiospore initiation in *Ustilago maydis*. Can. J. Bot. 58, 1548–1561.
Ronquist, F., Huelsenbeck, J.P., 2003. MRBAYES 3: Bayesian phylogenetic inference under mixed models. Bioinformatics 19, 1572–1574.
Rozen, S., Skaletsky, H.J., 2000. Primer3 on the WWW for general users and for biologist programmers. In: Krawetz, S., Misener, S. (Eds.), Bioinformatics Methods and Protocols: Methods in Molecular Biology. Humana Press, Totowa, pp. 365–386.
Sambrook, J., Russell, D.W., 2001. Molecular Cloning: A Laboratory Manual. Cold Spring Harbour Laboratory Press, New York.
Saville, B.J. et al., 2012. Investigating host induced meiosis in a fungal plant pathogen. In: Swan, A. (Ed.), Meiosis – Molecular Mechanisms and Cytogenetic Diversity. Intech, Rijeka, pp. 411–460.
Sellam, A. et al., 2010. Role of transcription factor CaNdt80p in cell separation, hyphal growth, and virulence in *Candida albicans*. Eukaryot. Cell 9, 634–644.
Seto, A.M., 2013. Analysis of Gene Transcripts during *Ustilago maydis* Teliospore Dormancy and Germination. Environmental and Life Sciences, vol. M.Sc. Trent University, Peterborough, pp. 129.
Shuster, E.O., Byers, B., 1989. Pachytene arrest and other meiotic effects of the start mutations in *Saccharomyces cerevisiae*. Genetics 123, 29–43.
Snetselaar, K.M., Mims, C.W., 1992. Sporidial fusion and infection of maize seedlings by the smut fungus *Ustilago maydis*. Mycologia 84, 193–203.
Stothard, P., 2000. The sequence manipulation suite: JavaScript programs for analyzing and formatting protein and DNA sequences. Biotechniques 28, 1102–1104.
Tamura, K. et al., 2011. MEGA5: molecular evolutionary genetics analysis using maximum likelihood, evolutionary distance, and maximum parsimony methods. Mol. Biol. Evol. 28, 2731–2739.
Tollot, M. et al., 2016. The WOPR protein Ros1 is a master regulator of sporogenesis and late effector gene expression in the maize pathogen *Ustilago maydis*. PLoS Pathog. 12 (6), e1005697. http://dx.doi.org/10.1371/journal.ppat.1005697.
Tung, K.S. et al., 2000. The pachytene checkpoint prevents accumulation and phosphorylation of the meiosis-specific transcription factor Ndt80. Proc. Natl. Acad. Sci. USA 97, 12187–12192.
Wang, J. et al., 1988. Gene transfer system for the phytopathogenic fungus *Ustilago maydis*. Proc. Natl. Acad. Sci. USA 85, 865–869.
Wang, J.S. et al., 2006. The DNA-binding domain of CaNdt80p is required to activate CDR1 involved in drug resistance in *Candida albicans*. J. Med. Microbiol. 55, 1403–1411.
Waterhouse, A.M. et al., 2009. Jalview Version 2 – a multiple sequence alignment editor and analysis workbench. Bioinformatics 25, 1189–1191.
Wheeler, M.H., 1983. Comparisons of fungal melanin biosynthesis in ascomycetous, imperfect and basidiomycetous fungi. Trans. Br. Mycol. Soc. 81, 29–36.
Xiang, Q., Glass, N.L., 2002. Identification of vib-1, a locus involved in vegetative incompatibility mediated by het-c in *Neurospora crassa*. Genetics 162, 89–101.
Xu, L. et al., 1995. NDT80, a meiosis-specific gene required for exit from pachytene in *Saccharomyces cerevisiae*. Mol. Cell. Biol. 15, 6572–6581.
Zahiri, A.R. et al., 2005. Differential gene expression during teliospore germination in *Ustilago maydis*. Mol. Genet. Genomics 273, 394–403.